In-situ real-time monitoring of spurious modes in HE_{11} transmission lines using multi-hole couplers in miter bends

Alexander Zach[1,*], *Walter* Kasparek[1], *Carsten* Lechte[1], *Burkhard* Plaum[1], *Francesco* Monaco[2], *Harald* Schütz[2], *Jörg* Stober[2], *Hiroshi* Idei[3], and *Thomas* Hirth[4]

[1]Institut für Grenzflächenverfahrenstechnik und Plasmatechnologie, Universität Stuttgart, Pfaffenwaldring 31, D-70569 Stuttgart, Germany
[2]Max-Planck-Institut für Plasmaphysik, Boltzmannstr. 2, D-85748 Garching, Germany
[3]Research Institute for Applied Mechanics, Kyushu University, Kasuga 816-8560, Japan
[4]Karlsruher Institut für Technologie, Kaiserstr. 12, D-76131 Karlsruhe, Germany

Abstract. Transmission of high-power millimeter waves for ECRH is often realised with oversized corrugated circular waveguides. Coupling from the gyrotron source to the waveguide is typically done via matching mirrors in free space. Small alignment errors of the system lead to the excitation of higher-order modes inside the waveguide beside the main transmission mode HE_{11}. Those modes have comparably higher losses and can in worst case result in local fields exceeding the breakdown limit of the medium inside the waveguide.
For alignment control over the whole pulse duration of the gyrotron, a set of hole-array couplers placed into a miter bend mirror probes the field inside the waveguide. The arrays are designed to detect the marker modes for beam offset and tilt ($LP_{11}^{(e/o)}$) as well as for beam waist mismatch (LP_{02}). In addition, a main mode coupler sensitive mostly for the HE_{11} content is used as a power monitor. By maximizing the signal of the power monitor and minimizing the content of marker modes, a first-order optimization of the coupling from free space to the waveguide can be achieved. Signal processing of the 140 GHz information is done at kHz range after downmixing, using a frequency shifted part of the power monitor signal.
As the measurement system is placed in a miter bend mirror, it can also be easily installed at various locations along the transmission line to check for possible misalignments of the waveguide connections between miter bends. Simulation and low power experimental results will be shown.

1 Introduction

An important problem in transmission of high-power millimeter waves for ECRH is to avoid spurious mode excitation in oversized corrugated circular waveguide (OCCWG) transmission lines. These modes have higher losses compared to the main transmission mode HE_{11} and can result in hot spots along the transmission line, which can also have influences on structure cooling demand. There are two main sources for spurious mode excitation that are related to misalignments. One is the coupling from the gyrotron millimeter wave source to the OCCWG, which is typically done with a matching optic consisting of two or more mirrors in free space. The other is mode conversion due to misalignments between OCCWG segments along the transmission line. Mode conversion at miter bends is another main source for spurious modes, but it can not be corrected by a better alignment.

The over 60 m long transmission lines at ASDEX Upgrade have a diameter of 87 mm each and are typically operated with up to 10 s pulses at 140 GHz and 1 MW in atmosphere. They are aligned with a laser system to an accuracy better than 1 mm. As the transmission line is not evacuated, miter bend mirrors can be easily exchanged, which gives the opportunity to place diagnostic systems at those positions. A spurious mode detector integrated in a miter bend mirror was developed to allow for faster, less complicated, and in-situ (re-)alignment. It can be used to confirm the alignment of OCCWG segments between two miter bend positions or to optimise the coupling from the gyrotron to the OCCWG.

Another use of the diagnostic system is as an in-situ real-time monitor of the mode purity in the transmission line, giving more information in comparison to using only power monitors. This covers also possible changes of beam parameters over the pulse duration, especially during the initial frequency chirp of the gyrotron due to thermal expansion of the cavity.

The following chapters describe the used method of mode detection and show results of the low power calibration for a prototype miter bend mirror diagnostic system.

2 Modes in the transmission line

In an OCCWG a couple of thousand modes can propagate. An estimated number in relation to the diameter D and the

*e-mail: zach@igvp.uni-stuttgart.de

free-space wavenumber k_0 is given by [1]:

$$(Dk_0)^2/8 \quad (1)$$

Linear polarized modes as described by Kowalski et al. [2] are used in this paper, as they directly relate to the most common misalignments.

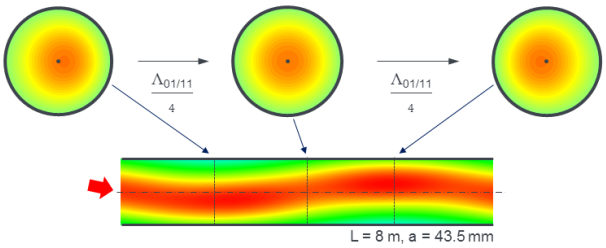

Figure 1. Resutling field in the OCCWG over a length of 8 m for a tilted input beam (0.15° tilted J_0 resulting in 98.8 % LP_{01} and 1.2 % LP_{11}).

The main transmission mode LP_{01} (or HE_{11}) propagates together with excited spurious modes forming an interference pattern inside the OCCWG. Fig. 1 shows such a pattern for an initially tilted beam composed of LP_{01} and LP_{11}. As the modes propagate with different wavenumbers

$$k_{mn} = k_0 \sqrt{1 - 4X_{mn}^2/(k_0 D)^2} \quad (2)$$

where X_{mn} is the n^{th} root of the m^{th} Besselfunction. The interference pattern after a quarter of the beat-wavelength corresponds to the maximum centroid offset.

Detection of the full spectrum of modes in an OCCWG would require information about amplitude and phase of the field over the whole cross section. But each kind of misalignment excites dominantly only a limited set of modes. In this paper they are hereinafter also called marker modes for that kind of misalignment. So a reduced mode spectrum for the detection of spurious modes due to misalignment can be assumed. The perturbations due to unconsidered modes scale with the residual power in those modes. The most important marker modes are shown in Fig. 2.

The LP_{11} modes are excited due to an offset or tilted input beam or such misalignments between OCCWG segments. For a gaussian beam input, also a minor amount of LP_{02} is excited. However, for small misalignments this effect is negligible and with corresponding small truncation losses the scaling of LP_{11} excitation is similar for offset and tilt as can be seen in Fig. 3 a). In the case of a mismatch between beam radius and waveguide diameter or a curved phase front at the OCCWG entrance the LP_{02} and LP_{03} modes are dominantly excited. For example, one can see the effect in low power 2D scans used for calibration such as in Fig. 3 b) and c). The field with 5 % LP_{02} content was created by moving the beam waist farther away from the input, thus creating a beam waist mismatch and a non-planar phasefront at the OCCWG input. In both settings some small amounts of other spurious modes are also present, as the generation of fields for the low power calibration was not done independently for each mode.

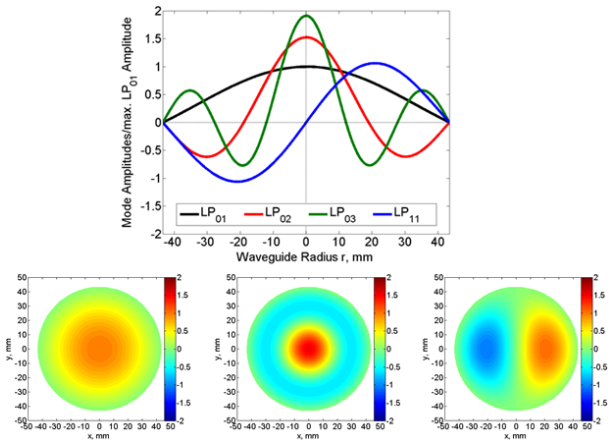

Figure 2. Mode amplitudes in the OCCWG cross section at y = 0 (top) and 2D amplitude distribution of main transmission mode LP_{01} (bottom left) and marker modes for LP_{02} (bottom mid, beam waist mismatch) and LP_{11}^{o} (bottom right, offset/tilt). Even first mode indices (m) relate to symmetric, odd first indices to asymmetric modes.

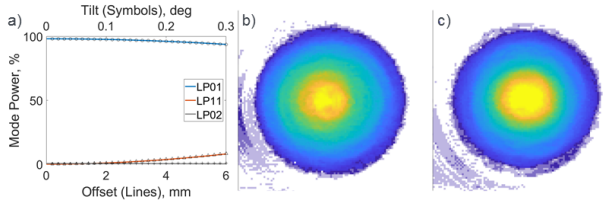

Figure 3. a) Mode content of LP_{01}, LP_{02}, and the dominantly excited spurious mode LP_{11} for an either tilted (symbols) or offset (lines) gaussian input beam. For negligible beam truncation, the values can also be related to the points of maximum tilt or offset in Fig. 1. b) Linear amplitude of 2D field scan with approx. 0.5 % LP_{02} content. c) Linear amplitude of 2D field scan with approx. 5 % LP_{02} content.

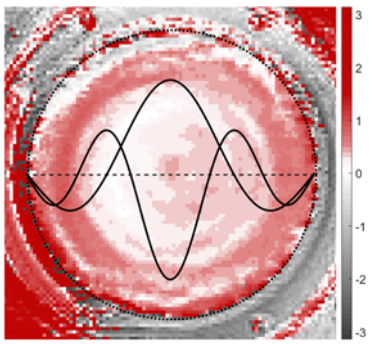

Figure 4. Phase of 2D field scan with 0.6 % LP_{02}, 0.4 % LP_{03}, and 2.7 % LP_{11}^{o} content (enhanced color scheme).

For strong misalignments, one can see the mode structure directly in the phase. In the phase plot in Fig. 4 one can see a ring of different phase that corresponds to the LP_{02} and LP_{03} modes, which have a phase offset to the main transmission mode LP_{01} of 36° and -66° respectively. A phase tilt between left and right which corresponds to

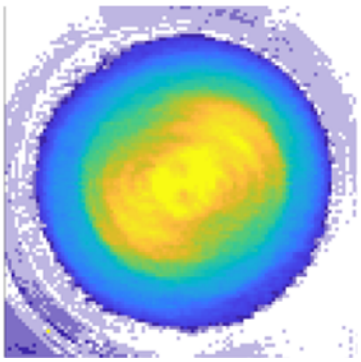

Figure 5. Linear amplitude of 2D field scan with approx. 1 % LP_{21}^{e} content (scaling factor $\sqrt{2}$ compared to Fig. 3).

the LP_{11}^{o} mode can also be seen. The field in Fig. 5 shows the result of an astigmatic input beam. The correspondent excited modes are the LP_{21} modes.

3 Detection of spurious modes in the transmission line

The field in the OCCWG cross section is sampled with hole couplers, which are integrated into a miter bend mirror. At 140 GHz the holes are in cut-off. This results in signal damping by about 60 dB. The signals are coupled to fundamental mode waveguides beneath the mirror surface as illustrated in Fig. 6. The detected signal of one channel is composed of coupling from several holes to the same waveguide, as

$$S = \sum_{H} A_H \, C_H \, e^{-ik_{mn}d_H} \, e^{-ik_g z_H} \tag{3}$$

where A_H is the field amplitude at the hole, C_H is the hole coupling factor, $e^{-ik_{mn}d_H}$ is the factor accounting for the propagation in front of the mirror surface and $e^{-ik_g z_H}$ for the propagation inside the fundamental mode waveguide from the hole to the detector. Directivity is achieved when hole signals coherently add up due to the phase velocity inside the fundamental mode waveguide being matched to the free space propagation in front of the mirror surface. This is done by matching the Brillouin angle of the fundamental mode waveguide (for reference see [1]) to the angle of incidence ($\theta = 45°$)

$$\theta = \cos^{-1}\left(\sqrt{1-\left(\frac{\lambda_0}{2a}\right)^2}\right). \tag{4}$$

Additionally, a correction of the waveguide depth a must be made for H-plane couplers (coupling through narrow waveguide wall) to account for a broadening effect in the fundamental mode waveguide due to the holes. This type of couplers has been used as power monitors for many years [3]. They are also compatible with water cooling channels integrated into the same mirror.

3.1 Interferometric detection

For a high power test, opposite couplers in a cross-like configuration were connected in a simple interferometric

Figure 6. Schematic of the coupling from OCCWG cross section to the fundamental mode waveguide behind the mirror surface. The waveguide depth is matched for the single hole contributions to coherently add up.

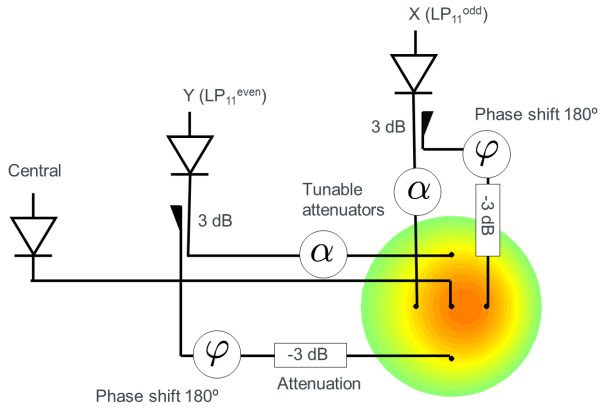

Figure 7. Schematic of an interferometric setup to measure direct error signals corresponding to the LP_{11} modes from coupled channels.

setup (see Fig. 7). If the connected channels are substracted, they detect the LP_{11} modes as the contributions of the symmetric modes (LP_{0n}, LP_{21}) cancel each other out.

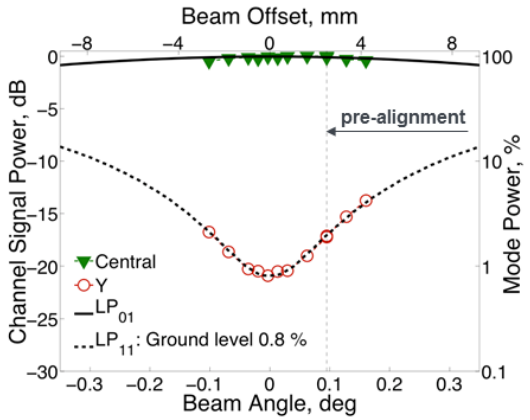

Figure 8. Measured signals and theoretical predictions for a simple interferometer setup. Beam offset and angle are coupled in this measurement.

The measurements were done in the ECRH-2 installation of ASDEX Upgrade. The miter bend with the couplers was installed instead of an already existing bend in the waveguide transmission line. The spurious modes were generated by tilting only one of the matching optic mirrors. That means the possible improvement of the

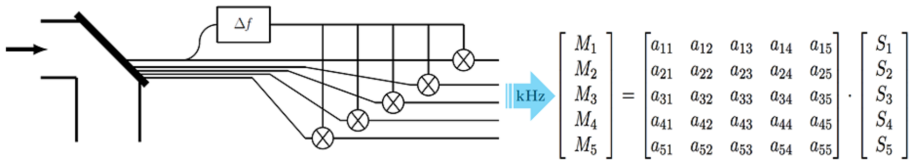

Figure 9. Schematic for the analysis of individual coupler signals

alignment was limited by the coupled tilt and offset of the input beam. The gyrotron power was 0.5 MW with pulse lengths up to 400 ms. Fig. 8 shows the measured signals along with theoretical predictions. A good agreement to the maximum signal from the center channel can be seen. Before the start of the measurements there was just a rough pre-alignment wih an LCD-target, so it does not indicate the accuracy of the mentioned laser adjustment at ASDEX Upgrade (see Sect. 1).

However, such an interferometric system gives no direct information wether the input beam is tilted or offset. Fine-alignment would have to be done interatively. For the detection of other modes (e.g., LP_{02}) an interferometric setup becomes very complicated and difficult to calibrate. Another way is to directly measure amplitude and phase of the single channels.

3.2 Analysis of Individual Coupler Signals

By implementing a heterodyne signal processing, the operating frequency of 140 GHz can be downmixed to a few kHz. The signals can then be directly measured with an oscilloscope and the mode powers can be calculated via a coefficient matrix obtained from the calibration. The schematic in Fig. 9 illustrates the realised method. One part of one channel signal is frequency shifted by reflection on a rotating grating and used as a local oscillator. The local oscillator signal is then split and coupled to the other signals and back to itself. After mixing at detection diodes, one obtains signals with the intermediate frequency in the kHz range. The phase of the downmixed signals is preserved.

4 Multiport Coupler Prototype

A prototype multiport coupler was designed and manufactured with some specification goals for spurious mode monitoring. It should directly detect the LP_{01} content on one of the channels by suppressing most of the marker modes for misalignment. The LP_{11} modes should be measured to determine offset and tilt of the input beam and the LP_{02} and LP_{21} modes should be measured. The system should also work with typical polarizations and have a bandwidth of at least 400 MHz.

The maximum hole diameter was set to $0.355\lambda_0$, because with larger hole diameters of $0.383\lambda_0$ arcing was observed at 0.6 MW during the high power test with the interferometric setup (see Sect. 3.1). Power monitors with $0.346\lambda_0$ hole diameters at the center of the OCCWG cross section are already successfully used at full power. The slightly larger maximum hole diameter is uncritical, as there are no such holes near the center, where the highest field strenghts are found. However the overall smaller holes for full power capability come at the cost of dynamic range for the low power calibration.

The manufactured prototye multiport coupler is shown in Fig. 10. It has three types of hole arrays. A main mode coupler accross the middle, two cross polarization couplers and four diagonal couplers. The symmetric layout was chosen to be able to use the multiport coupler in both directions in case of one direction giving better performance due to manufacturing tolerances.

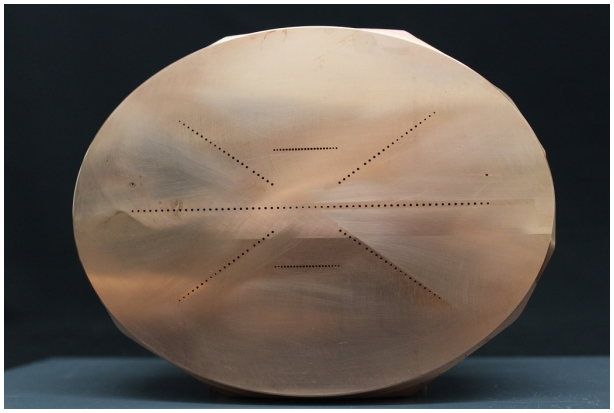

Figure 10. Coupling structures of a multiport coupler prototype.

4.1 Main mode coupler

The main mode coupler is designed to suppress all other LP_{0n} modes as well as all asymmetric modes (e.g., LP_{11}). Fig. 11 shows the suppression against the main mode for the coupler design. One has to keep in mind, that additionally the power in the spurious modes is typically at least 20 dB lower than in the main mode. Also one can see, that the suppression of the asymmetric modes is not as good, as for the LP_{0n} modes. This becomes clear, when looking at the coupling of the hole array in Fig. 12.

The coupling factors of the single holes are given by

$$C_H = r \cdot A(\,LP_{01}(r)\,) \tag{5}$$

where r is the distance from the cross section center and A is the amplitude of the LP_{01} mode at that position. The LP_{0n} mode coupling is suppressed along each side of the array, whereas the LP_{11}^{o} mode is strongly coupled on both the righthand and lefthand side and the suppresion

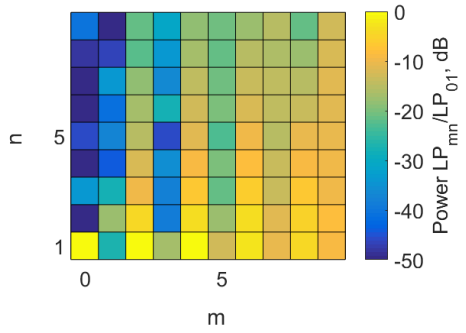

Figure 11. Calculated coupling suppression of spurious modes by the main mode coupler.

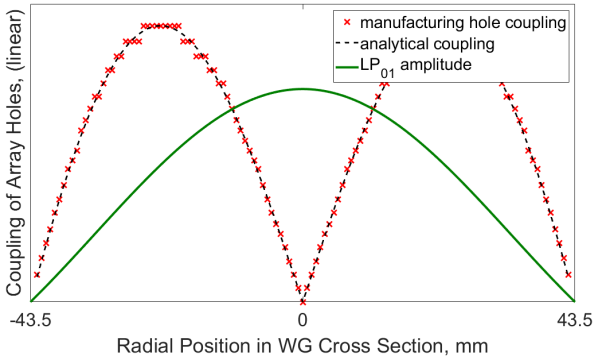

Figure 12. Coupling structure of main mode coupler.

results from the 180° phase difference between the two sides. However, one of the both signal parts has to also propagate through the other half of the array, being attenuated more and partly reflected. A compensation for this effect was neglected in order to keep symmetry and due to the manufacturing constraint of discrete hole diameters. The symmetric LP_{21} mode is very strongly coupled by the main mode coupler and has to be accounted for.

4.2 Cross polarization couplers

The cross polarization couplers are tapered E-plane couplers (coupling through broad waveguide wall) set at the position of the LP_{02} phase jump. Because for E-plane couplers the position of the hole in the fundamental mode waveguide wall has to be more exact than for H-plane couplers, no special mode sensitive coupling was attempted.

Fig. 13 shows a nice agreement between radiation angle measurements for which the prototype was placed on a rotating table and simulations of the individual coupling arrays with CST Microwave Studio [4] for both the main mode coupler and the cross polarization couplers. The strong response of the main mode coupler between the main peaks is related to reflections in the measurement setup.

4.3 Diagonal Couplers

The diagonal couplers utilize both waveguide ports by coupling in the forward as well as in the backward direc-

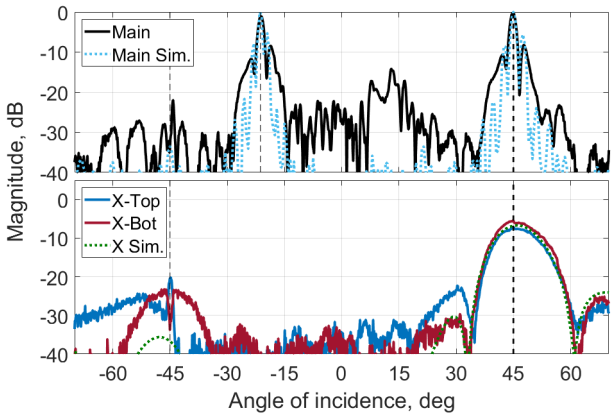

Figure 13. Radiation angle measurements and simulation for the main mode and the cross polarization couplers. At -45 degrees one can see the reflection of the main lobe due to non-perfect absorbtion at the other waveguide port. The second main lobe of the main mode coupler is related to the LP_{0n} suppression.

tion. The coupling structure is designed to have a high mode selectivity for LP_{01} and LP_{02} towards opposite ports. Fig. 14 shows the absolute amplitudes of these modes. The waveguide depth is chosen that all hole signals coherently add up in the forward direction (see Sect. 3). By having an equal total coupling for the LP_{02} on both sides of its phase jump, this mode is suppressed in the forward direction. Backwards coupling for the LP_{02} is achieved by a distance of half the waveguide wavelength between the holes and an additional quarter wavelength at the phase jump position.

The LP_{01} mode coupling in the backwards direction is suppressed by having also equal total coupling on both sides of the phase jump position for this mode. Because such arrays have a high reflection for propagating waves in the fundamental mode waveguide, the coupling was also optimised to behave similar for both orientations of the array towards the field in the OCCWG (wether the first hole to couple is near the middle or on the outside of the cross section).

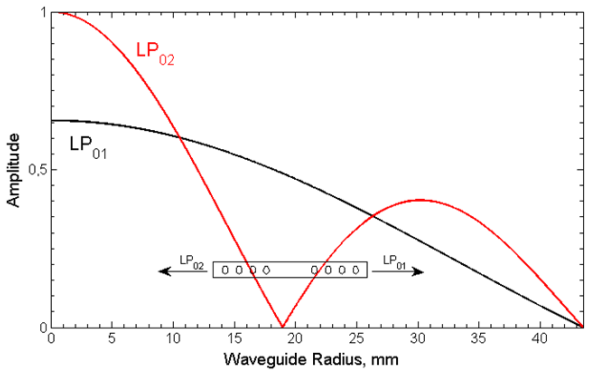

Figure 14. Absolute amplitude of the LP_{01} and LP_{02} mode showing the possibility of mode sensitive coupling in opposite directions inside the fundamental mode waveguide.

When looking at the transmission characteristics through the fundamental mode waveguides of the diagonal couplers, one can see in Fig. 15 a shift by approximately 2.2 GHz compared to the simulation. It is not yet fully understood, but the most probable error is the manufactured waveguide depth being 1.269 mm instead of 1.296 mm. It was maybe manually set in the machining program after being changed from 1.311 mm in the drawing. However, a remaining low mode selectivity still allows for full diagnostic capability.

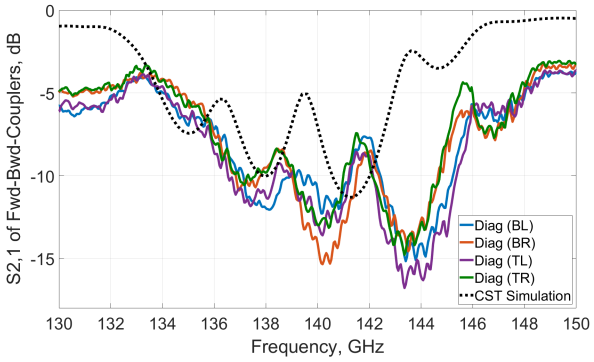

Figure 15. Transmission through the fundamental mode waveguides with the diagonal coupler structures. The simulation does not account for attenuation outside of the coupling structure region.

5 Low power results

The multiport coupler prototype diagnostic system was assembled and tested at low power (see Fig. 16). In preparation for high power tests, a calibration with 9 used ports and 9 different vertically polarized field configurations was performed. For additional tested field configurations a good agreement between the mode analysis of 2D scans and the results obtained from the multiport coupler is found (see table 1). An expected larger phase offset error at low mode power is observed. The minimum detectable LP_{11} content is limited to 0.2 % mostly by the accuracy of the 2D scans. This corresponds to a maximum offset of 0.9 mm in the beat pattern described in Sect. 2 and is in the same range as the laser adjustment.

As an example, one of the 2D scans is shown in Fig. 17. One can clearly see the offset and tilt corresponding to the large LP_{11} content in the amplitude and phase plot respectively.

6 Conclusions

A high power capable in-situ diagnostic tool for spurious modes due to misalignments in OCCWGs has been developed. Low power tests show promising results and high power tests are scheduled.

Table 1. Mode powers and phase differences from 2D scan mode analysis and multiport coupler measurements (MPC) for two tested field configurations. The LP_{21} modes are not shown, because their mode content is less than 0.2 %.

	2D (1)	MPC (1)	2D (2)	MPC (2)
LP_{01}	92.65 %	92.58 %	91.98 %	92.11 %
LP_{02}	0.43 % 1.5°	0.54 % -0.6°	0.16 % 12.2°	0.16 % 4.9°
LP_{03}	0.42 % -58.1°	0.35 % -68.3°	0.39 % -60.0°	0.29 % -60.4°
LP^{e}_{11}	4.59 % -15.5°	4.66 % -15.0°	0.18 % -26.1°	0.20 % -28.6°
LP^{o}_{11}	0.61 % -170.6°	0.69 % -181.2°	5.72 % -24.9°	5.60 % -24.7°

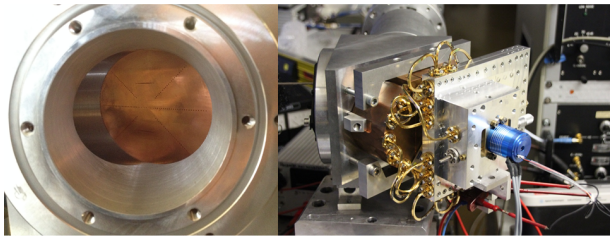

Figure 16. Assembled multiport coupler prototype diagnostic system consisting of the multiport coupler and the waveguide based signal processing unit. This unit is using a rotating grating and a coupling plate with integrated Talbot effect splitter as illustrated in Fig. 9.

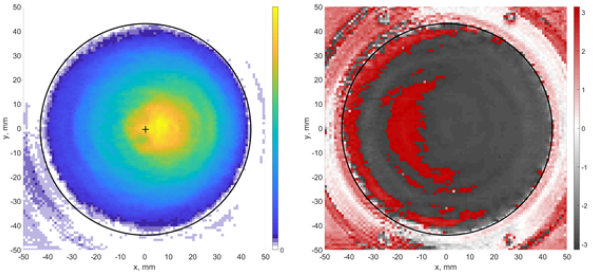

Figure 17. 2D scan with linear scaling of a field with a large LP^{o}_{11} content corresponding to (2) of table 1.

References

[1] H.-J. Hartfuss and T. Geist, *Fusion Plasma Diagnostics with mm-Waves - An Introduction* (Wiley-VCH, Weinheim (Germany), 2013) p177

[2] E. J. Kowalski et al., IEEE Trans. Microw. Theory Tech. **58**, 2772-2780 (2010)

[3] D. Wagner et al., J Infrared Millim Terahertz Waves **32**, 274-282 (2011)

[4] www.cst.com/products/cstmws